Received: 17 February 2024 | Revised: 26 June 2024 | Accepted: 2 July 2024

DOI: 10.1111/joa.14113

Journal of Anatomy ANATOMICAL SOCIETY WILEY

ORIGINAL ARTICLE

The evolution of the air sac system in theropod dinosaurs: Evidence from the Upper Cretaceous of Madagascar

Tito Aureliano[1,2] | Waltécio Almeida[1] | Masinissa Rasaona[2,3] | Aline M. Ghilardi[1,2]

[1]Laboratory of Zoology, Department of Biological Chemistry, Programa de Pós-Graduação em Diversidade Biológica e Recursos Naturais, Regional University of Cariri (URCA), Crato, Brazil

[2]Diversity, Ichnology and Osteohistology Laboratory (DINOlab), Department of Geology, Federal University of Rio Grande Do Norte (URFN), Natal, Brazil

[3]Mention Bassins Sédimentaires, Evolution, Conservation, University of Antananarivo (UA), Antananarivo, Madagascar

Correspondence
Tito Aureliano, Laboratory of Zoology, Department of Biological Chemistry, Programa de Pós-Graduação em Diversidade Biológica e Recursos Naturais, Regional University of Cariri (URCA), Crato, Brazil.
Email: tito@dinolab.science

Funding information
Fundação Cearense de Apoio ao Desenvolvimento Científico e Tecnológico, Grant/Award Number: FUNCAP/FPD-0213-00295.01.01/23; Fundação Norte-Rio-Grandense de Pesquisa e Cultura, Grant/Award Number: FUNPEC-UFRN/PIB21712-2023

Abstract

Recent evidence suggests that the invasive air sac system evolved at least three times independently in avemetatarsalians: in pterosaurs, sauropodomorphs and theropods. Data from sauropodomorphs showed that the pneumatic architecture in vertebrae first developed in camellate-like trabeculae in the Triassic, later in camerate systems in Jurassic neosauropods, and finally camellate tissue in Cretaceous titanosaurs. This evolutionary trajectory has support from a considerable sampling of sauropodomorph taxa. However, the evolution of pneumatic bone tissues in Theropoda is less understood. We analyzed the computed tomography of *Majungasaurus* and *Rahonavis*, using densitometry rendering to differentiate the microarchitecture along the presacral axial skeleton of late Ceratosaurians and early Paravians. We also compared these results with scans of other theropod clades. Our analysis revealed an increase in pneumatic complexity in early paravians compared to the ceratosaurians. *Majungasaurus* presents some apneumatic neural spines, a condition also observed in *Allosaurus*. *Majungasaurus* also features some apneumatic centra despite the presence of lateral pneumatic fossae. This raises caution when evaluating PSP solely based on external morphology. We also found evidence of distinct patterns of PSP in maniraptorans. Considering that *Majungasaurus*, a late abelisaurid, inherited from their ceratosaurian ancestors, some apneumatic elements such as the neural spine and some centra, *Rahonavis*, an early paravian, took a different trajectory toward the full pneumatization of the axial skeleton. This characteristic provided paravians an advantage in gliding and flying. Also, unlike Sauropoda, pneumaticity in Theropoda apparently developed by increasing chamber volumes toward paravians. Similar studies on early Theropoda are needed to elucidate their condition and better describe the evolutionary trajectory of different groups.

KEYWORDS
Africa, computed tomography, Dinosauria, morphology, respiratory system, vertebrae

1 | INTRODUCTION

Theropods comprehend the longest-living and the only surviving clade of dinosaurs with an evolutionary history spanning over 200 million years (Cuesta et al., 2015; Malafaia et al., 2018; Müller, 2021; O'Connor & Zhou, 2015; Rayfield, 2005; Zanno & Makovicky, 2011). One of the key aspects of their success relies on the agile lightweight bodies with high oxygen supply capable of explosive pursuits, and even flight in some clades (Britt, 1994; Britt et al., 1998; Wedel, 2009). This adaptation resulted from the

unique unidirectional breathing maximized by the evolution of the diverticula that extends from the lungs (Maina, 2005; Proctor & Lynch, 1993). Most of these air sac systems invade the axial skeleton and pneumatize the bone tissue, following blood irrigation pathways along ontogeny (Maina, 2006; Taylor & Wedel, 2021). The detection of unambiguous postcranial skeletal pneumaticity (PSP) is the standard method to infer the presence of air sacs in fossil organisms (O'Connor, 2006). This method consists of detecting the conjoint presence of an external pneumatic foramen connecting with internal camerae or camellae. Earlier hypotheses based on sauropod vertebrae indicated the evolution of the internal pneumatic chambers evolved from larger camerae into smaller camellae, from early neosauropods to the late titanosaurs (Wedel, 2003; Wedel et al., 2000). Recent evidence from the earliest sauropodomorphs in the Carnian found apneumatic skeletons in *Buriolestes* and *Pampadromaeus* and delicate camellate-like pneumatic protocamerate trabeculae in the Norian unaysaurid *Macrocollum* (Aureliano et al., 2022, 2023). These finds suggested a new view on the evolution of the pneumatic architectures in sauropodomorphs, that may have evolved from delicate trabecular arrangements in the Triassic to larger chambers in the Jurassic, toward a delicate arrangement again in the Late Cretaceous (Aureliano et al., 2023). Nonetheless, it is uncertain whether the same pattern is valid for non-avian theropods since fewer studies have been conducted (Aranciaga Rolando et al., 2020; Baiano et al., 2023; Britt, 1994; Britt et al., 1998; Brum et al., 2018; Forster et al., 2020; Gianechini & Zurriaguz, 2021; Iori et al., 2021; O'Connor, 2007; Poropat et al., 2020; Smith et al., 2021; Watanabe et al., 2015). In this study, we analyzed the presacral axial skeletons of the ceratosaurian *Majungasaurus* (Lavocat, 1955; O'Connor, 2007) and the early paravian *Rahonavis* (Forster et al., 1998a, 1998b), from the Upper Cretaceous Maevarano Formation, NW Madagascar, using computed tomography to detect different patterns of pneumatization and discuss the evolution of PSP in theropods.

2 | MATERIALS AND METHODS

2.1 | Institutional abbreviations

AMNH, American Museum of Natural History, New York, United States; AzMNH, Arizona Museum of Natural History, Mesa, Arizona, USA; CAPPA/UFSM, Centro de Apoio à Pesquisa Paleontológica da Quarta Colônia, Universidade Federal de Santa Maria, Rio Grande do Sul, Brazil; LPP-PV, Laboratório de Paleoecologia e Paleoicnologia (UFSCar), Federal University of São Carlos (UFSCar), São Paulo state, Brazil; MPM, Museo Regional Provincial 'Padre Manuel Jesús Molina', Río Gallegos, Argentina; MPMA, Museu Paleontológico de Monte Alto, Monte Alto, São Paulo state, Brazil; OMNH, Oklahoma Museum of Natural History, Oklahoma, United States; UA, Ohio University, United States; UCMP, University of California Museum of Paleontology, Berkeley, California, USA; ULBRA, Centro de Apoio à Pesquisa Paleontológica da Quarta Colônia, Universidade Federal de Santa Maria, São João do Polêsine, Rio Grande do Sul, Brazil (previously Museu de Ciências Naturais, Universidade Luterana do Brasil, Canoas, Brazil); UMNH-VP, Natural History Museum of Utah, Utah Museum of Natural History Vertebrate Paleontology, Salt Lake City, Utah, USA; USNM, Smithsonian Institution, National Museum of Natural History, Washington DC, USA.

2.2 | Specimens

The specimen of *Majungasaurus crenatissimus* (UA 8678) analyzed in this study corresponds to a moderately complete skeleton and one of the best-preserved abelisaurids (O'Connor, 2007). It was one of the latest ceratosaurians and the top predator of its ecosystem. The holotype of *Rahonavis ostromi* (UA 8656), in turn, corresponds to a partial postcranial skeleton, with one cervical, a few dorsal, and several caudal vertebrae associated with appendicular elements (Forster et al., 1998a, 1998b). The histological analysis of *Rahonavis* UA 8656 is consistent with a somatically mature individual (Forster et al., 2020). There is no histological analysis available for *Majungasaurus* UA 8678, but O'Connor (2007) notes it was likely a sub-adult individual; hence, nearly all of the neural arches and associated centra are unfused. We analyzed the cervical and dorsal elements of both specimens in this study (UA 8678: C7, C10, D2, and D5; UA 8656: posterior cervical, anterior dorsal, posterior dorsal).

2.3 | Locality and horizon

For the past 30 years, several expeditions have been carried out at the Berivotra fossil site in the Mahajanga Basin. From 1993 to the present day, these expeditions resulted from the joint partnership between the University of Stony Brook (New York, United States) and the University of Antananarivo (Madagascar) under the Mahajanga Basin Project (Forster et al., 2020; Krause et al., 2022). The specimen *Majungasaurus crenatissimus* (UA 8678) was found at the olive-green clayey sandstone, Berivotra Site locality MAD 96–21 (Madagascar Collection, coordinates: −15°54′ 29.09″ S, 46°34′ 55.2″ E). The holotype of *Rahonavis ostromi* (UA 8656), in turn, was found in the mudstone at the locality MAD 93–18 (Madagascar Collection, coordinates: −15°54′ 9.26″ S, 46°34′ 42.43″ E). Both outcrops are near the Berivotra village (Figure 1), District of Maevarano, Boeny Region, northwestern Madagascar (Rogers et al., 2000; Sampson & Witmer, 2007). These two sites are part of Anembalemba member, Upper Cretaceous (Campanian to Maastrichtian), Maevarano Formation, Mahajanga Basin (Fanti & Therrien, 2007; Krause et al., 2007, 2022; Rogers et al., 2000).

2.4 | Taphonomic remarks

Specimens are well-preserved overall, but cracks and fractures are present throughout the *Majungasaurus* UA 8678 and *Rahonavis* UA

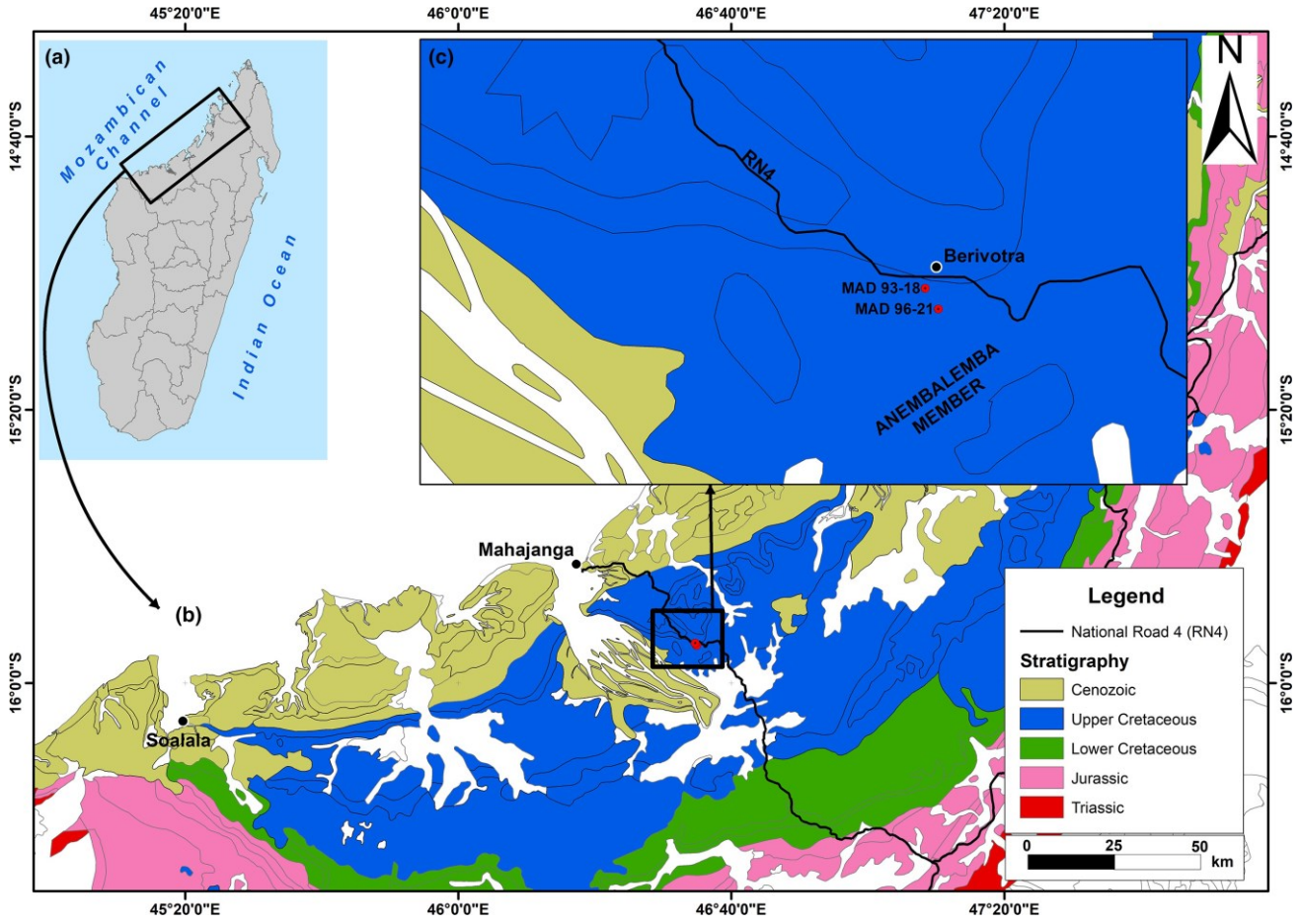

FIGURE 1 (a) Map of Madagascar and the Mahajanga Basin location. (b) Details of the basin and the location of the Berivotra study area. (c) The black box highlights the area of study of the Mahajanga Basin Project, the site where the fossils of this study were collected under the Upper Cretaceous Maevarano Formation context. Adapted from Besairie (1969).

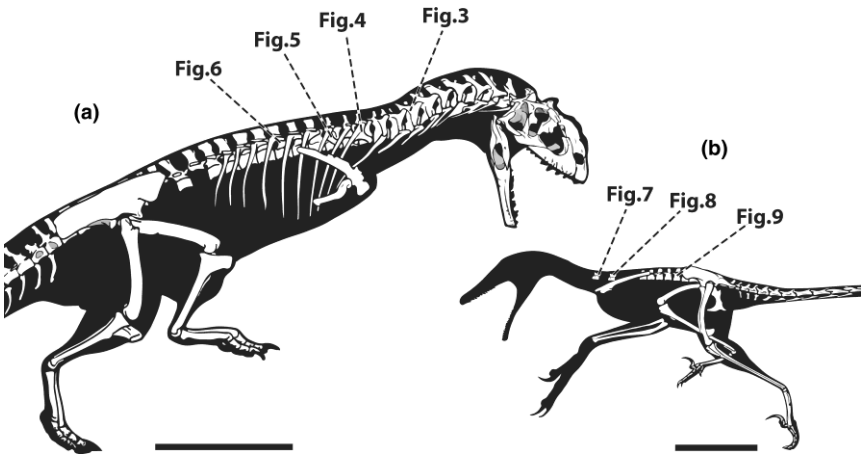

FIGURE 2 Index of analyzed specimens and vertebrae. (a), The abelisaurid *Majungasaurus crenatissimus* (UA 8678). (b), The paravian *Rahonavis ostromi* (UA 8656). Scale bar in a = 1000 mm and in b = 100 mm. Skeletal reconstructions adapted from Jaime A. Headden (https://creativecommons.org/licenses/by-nc-sa/3.0/).

8656 vertebral series. Larger portions of the neural arch are missing in some elements of *Rahonavis* UA 8656. Nonetheless, the internal trabecular architectures are well-preserved, except for some localized areas in the centra of UA 8678 and neural arches of UA 8656.

2.5 | Anatomical nomenclature

We followed Wilson's nomenclature for vertebral fossae and laminae (Wilson, 1999, 2012; Wilson et al., 2011) Wedel's, O'Connor's, and Aureliano's works for the terminologies and description of unambiguous vertebral pneumatic structures (Aureliano et al., 2021; O'Connor, 2006; Wedel, 2003, 2007; Wedel et al., 2000).

2.5.1 | Anatomical abbreviations

acdl, anterior centrodiapophyseal lamina; c, centrum; cc, circumferential chambers; cdf, centrodiapophyseal fossa; cdl, centrodiapophyseal lamina; cprl, centroprezygapophyseal lamina; d, diapophysis; nc, neural canal; nc, neurocentral suture; par, parallel layers of trabecular bone; pc, pneumatic chamber; pcdl, posterior centrodiapophyseal lamina; pf, pneumatic foramen; po, postzygapophysis; pocdf, postzygapophyseal centrodiapophyseal fossa; podl, postzygapophyseal diapophyseal lamina; pr, prezygapophysis; prcdf, prezygapophyseal centrodiapophyseal fossa; rad, radial canals; s, neural spine; sdf, spinodiapophyseal fossa; spof, spinopostzygapophyseal fossa.

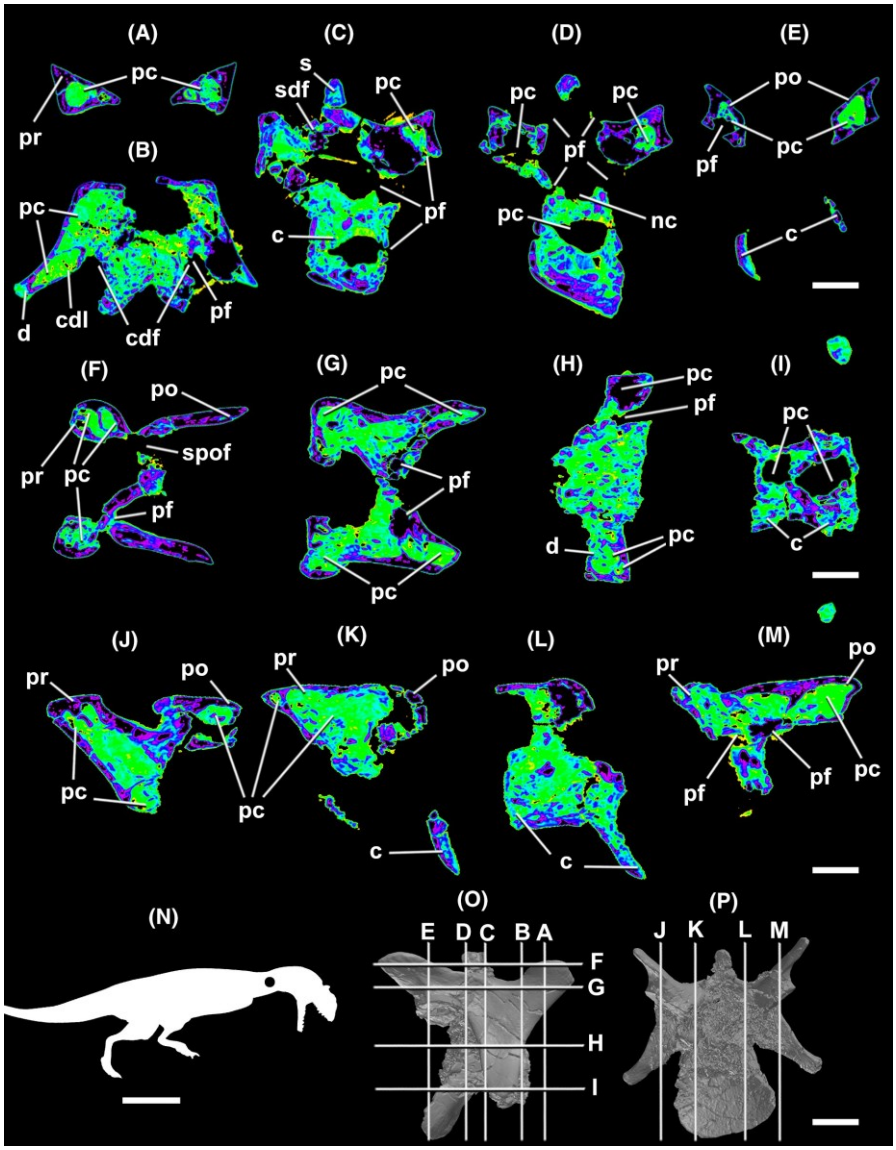

FIGURE 3 CT scan of *Majungasaurus* (UA 8678) mid-posterior cervical vertebra (C7) in transverse (A–E), frontal (F–I), and parasagittal (J–M) selected sections. (N) Silhouette shows the position of the axial element. Lighter blue and green indicate lower densities (e.g., pneumatic cavities). Purple and darker blue demonstrate denser structures (e.g., bone tissue). Silhouette adapted from Jaime Headden (https://creativecommons.org/licenses/by-nc-sa/3.0/). Three-dimensional reconstruction of the vertebra and the correspondent slices in lateral (O) and proximal (P) views. Scale bar in A-M,O,P = 20 mm and in N = 1000 mm.

2.6 | Computed tomography (CT scan)

The CT scan of *Majungasaurus* elements was published in O'Connor (2007). Data were uploaded to the Morphosource platform and are available through this link: https://www.morphosource.org/concern/biological_specimens/000461100. Protocols for the μCT scan of *Rahonavis* vertebrae are present in Forster et al. (2020). Data are available through this link: https://www.morphosource.org/concern/biological_specimens/000S23771. In this current study, we reanalyzed scans of the UA 8678 and UA 8656 vertebral series (Figure 2) using densitometry in rainbow color rendering following Aureliano's method (Aureliano et al., 2020, 2021). This method converts X-ray intensity dot matrix into a color range, highlighting different types of bone tissues and facilitating the microanatomical differentiation between compacta, spongiosa, and infilled rock minerals. We used 3D Slicer version 5.2.1 for the tomography analyses (Fedorov et al., 2012).

3 | RESULTS

The CT scan densitometry analyses provided novel insights into the vertebral microanatomy of *Majungasaurus* (Figures 3–6) and *Rahonavis* (Figures 7–9). Overall, taphonomic artifacts (e.g., cracks, mechanic fragmentation of trabeculae) did not affect the description of the internal architecture and allowed the detailed observation of fossae, laminae, and pneumatic foramina throughout the vertebral series.

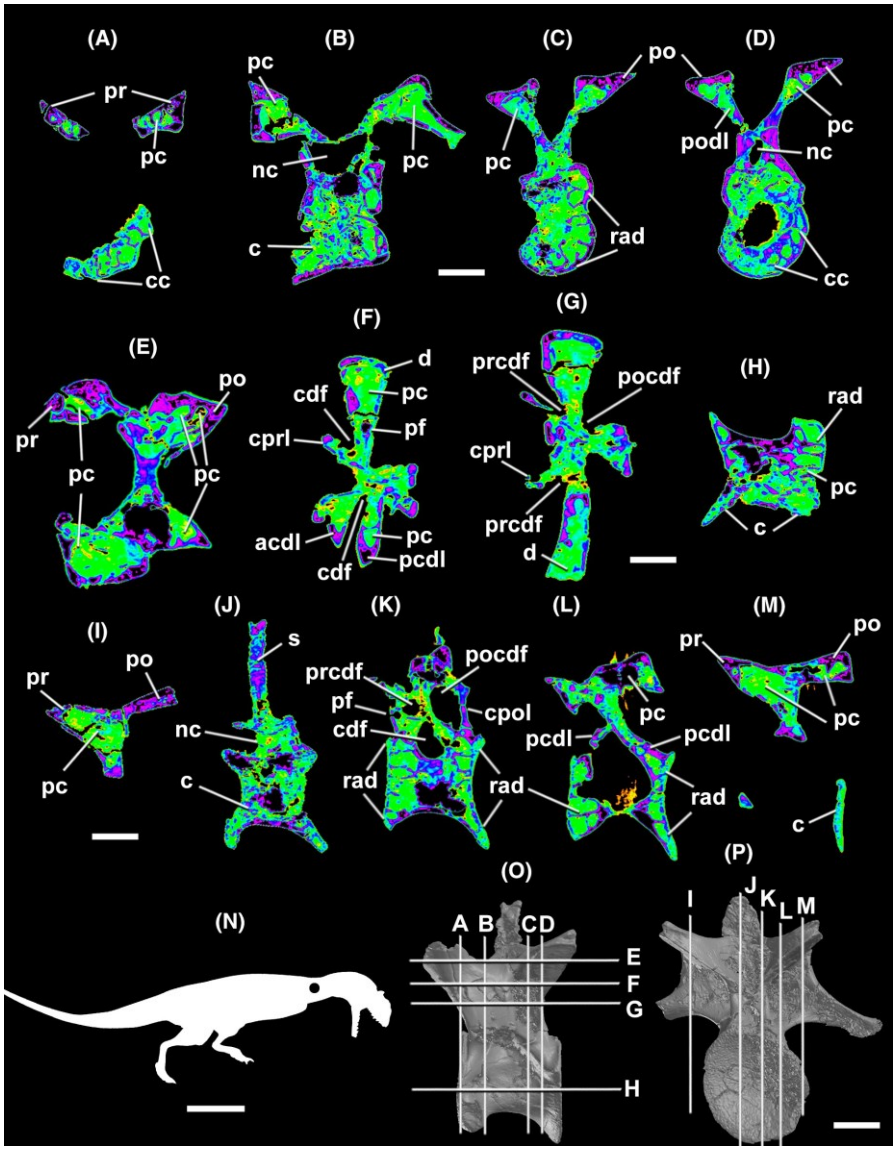

FIGURE 4 CT scan of *Majungasaurus* (UA 8678) posterior cervical vertebra (C10) in transverse (A–D), frontal (E–H), and parasagittal (I–M) selected sections. (N) Silhouette shows the position of the axial element. Lighter blue and green indicate lower densities (e.g., pneumatic cavities). Purple and darker blue demonstrate denser structures (e.g., bone tissue). Silhouette adapted from Jaime Headden (https://creativecommons.org/licenses/by-nc-sa/3.0/). Three-dimensional reconstruction of the vertebra and the correspondent slices in lateral (O) and proximal (P) views. Scale bar in A–M,O,P = 20 mm and in N = 1000 mm.

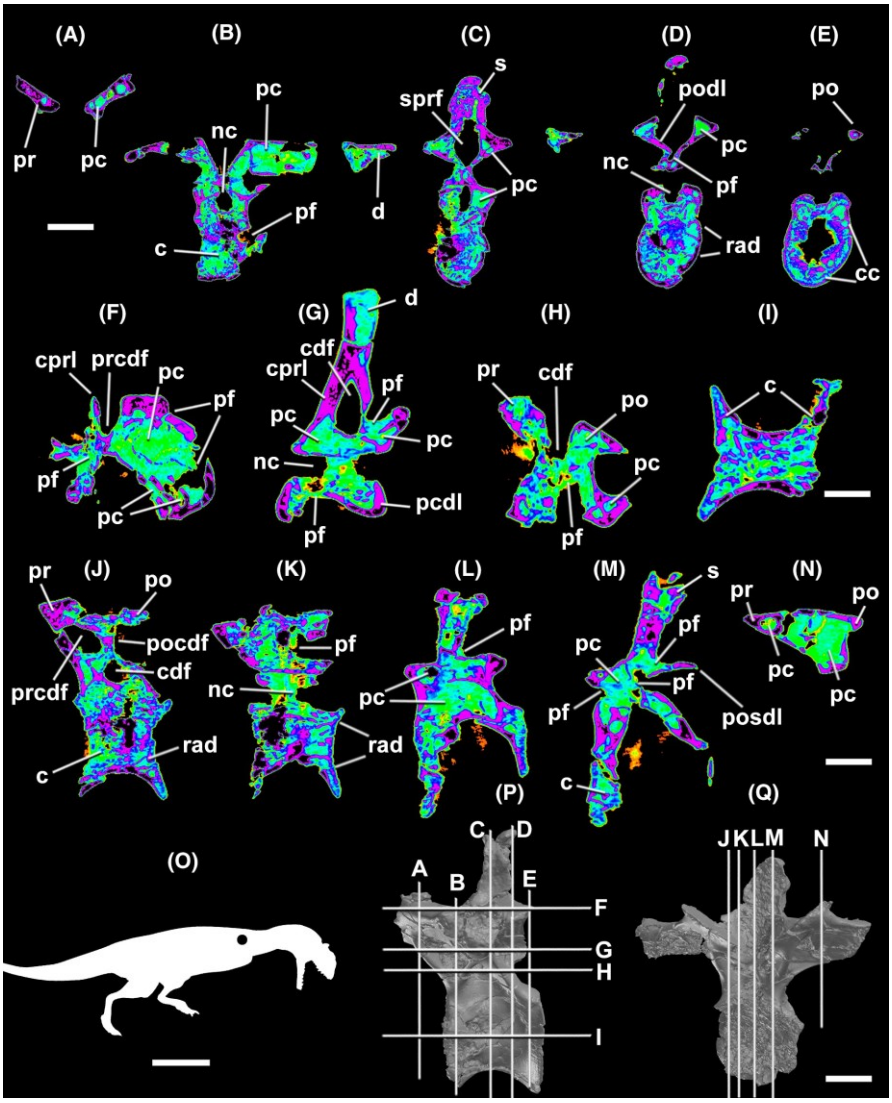

FIGURE 5 CT scan of *Majungasaurus* (UA 8678) anterior dorsal vertebra (D2) in transverse (A–E), frontal (E–H), and parasagittal (I–M) selected sections. (O) Silhouette shows the position of the axial element. Lighter blue and green indicate lower densities (e.g., pneumatic cavities). Purple and darker blue demonstrate denser structures (e.g., bone tissue). Silhouette adapted from Jaime Headden (https://creativecommons.org/licenses/by-nc-sa/3.0/). Three-dimensional reconstruction of the vertebra and the correspondent slices in lateral (P) and proximal (Q) views. Scale bar in A–N,P,Q = 20 mm and in O = 1000 mm.

3.1 | Pneumatic structures in *Majungasaurus* vertebrae

The posterior cervical vertebrae of *Majungasaurus* present deep fossae and well-defined laminae in the neural arches and a broad lateral foramen in the C10. Likewise, dorsals D2 and D5 also present deep fossae and well-defined laminae in the neural arches with a deep lateral foramen in D2 (absent in D5). The internal structures of the neural arch are strongly pneumatized with the predominance of polycamerate arrangements in both cervical and dorsal elements. The prezygapophyses and postzygapophyses present two to three internal chambers throughout the presacral series. Their architecture expands into several larger chambers resembling a butterfly dorsally in cervical and anterior dorsal vertebrae (Figures 3G, 4E and 5H). However, the cervical and dorsal neural spines present dense apneumatic trabecular bone (Figures 4J, 5C and 6D,E), except in the mid-cervical C7 (Figure 3C). The centra show small chambers that decrease complexity from the C7 to D5. C10 presents circumferential chambers ventrally (see cc in Figures 4A,C and 5E). C10 and D2 have camellate bone which projects radially from the inner centrum cortical walls (see rad in Figures 4C,H,K,L and 5D,J,K). D5 has a dense apneumatic trabecular array throughout the centrum (Figure 6), despite a large foramen laterally (Figure 6K,M).

3.2 | Pneumatic structures in *Rahonavis* vertebrae

The posterior cervical vertebra of *Rahonavis* presents deep fossae and well-defined laminae in the neural arch and broad lateral

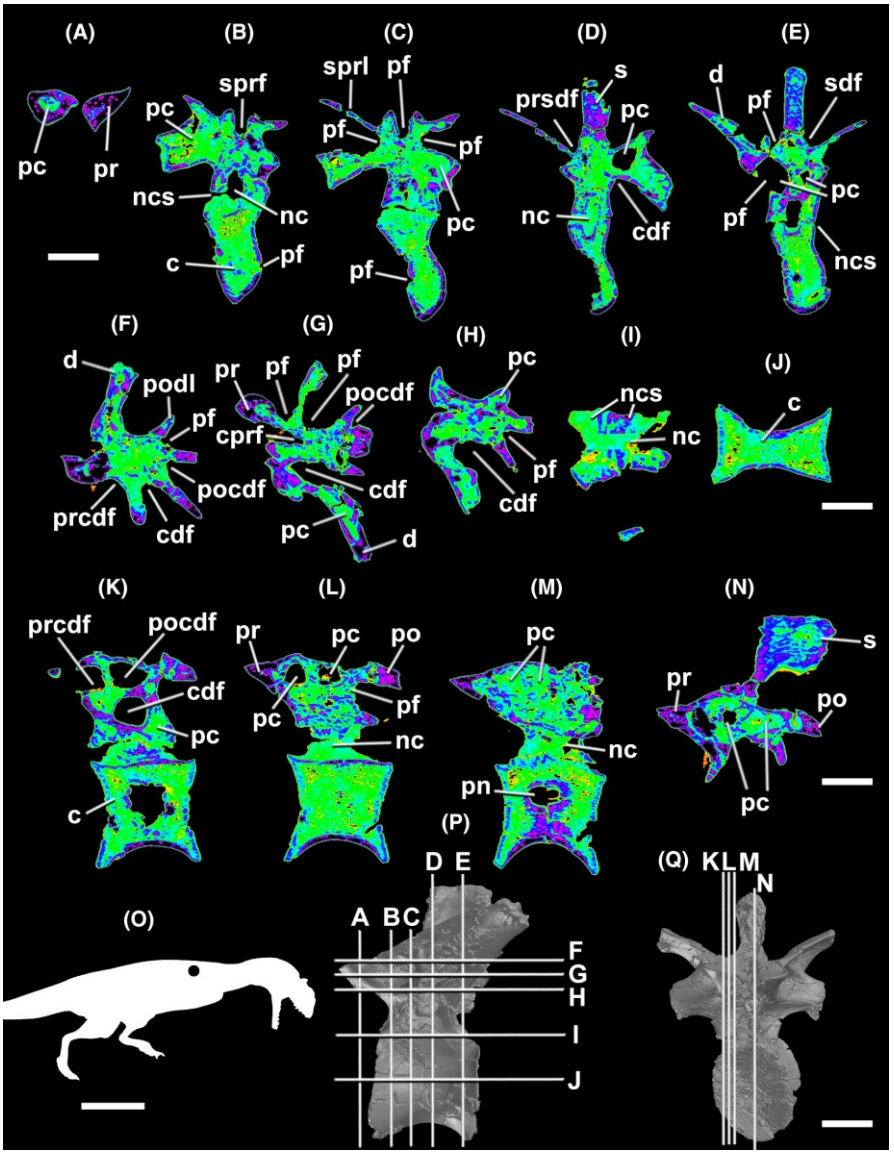

FIGURE 6 CT scan of *Majungasaurus* (UA 8678) mid-dorsal vertebra (D5) in transverse (A–E), frontal (F–J), and parasagittal (K–N) selected sections. (O) Silhouette shows the position of the axial element. Lighter blue and green indicate lower densities (e.g., pneumatic cavities). Purple and darker blue demonstrate denser structures (e.g., bone tissue). Silhouette adapted from Jaime Headden (https://creativecommons.org/licenses/by-nc-sa/3.0/). Three-dimensional reconstruction of the vertebra and the correspondent slices in lateral (P) and proximal (Q) views. Scale bar in A–N,P,Q = 20 mm and in O = 1000 mm.

foramina. Similar lateral foramina are also present in the anterior and posterior dorsals. The anterior dorsal neural arch also shows deep fossae and well-defined laminae. Only the base of the neural arch has been preserved for the posterior dorsal element of *Rahonavis*, and it bears deep fossae between the zygapophyses and the non-preserved diapophysis. The entire inner structure of the cervical and dorsal vertebrae is pneumatized with large chambers surrounded by delicate trabecular walls (Figures 7–9). The centra present elliptical anteroposteriorly oriented elongated chambers molded by radial trabecular walls (Figures 7I,N, 8K,M and 9H,M). There are two parallel trabeculae layers covering the cotyles' inner surface in the posterior dorsal element (Figure 9G–I,L,M). The neural arches present larger chambers with lower complexity (Figures 7A,E,K,L, 8A,C,J,K,M and 9J). The anterior dorsal neural spine (the only preserved in the presacral series) is intensely pneumatized with elliptical chambers oriented ventrodorsally (Figure 8C,D).

4 | DISCUSSION

The microanatomy of the presacral series of *Majungasaurus* and *Rahonavis* revealed an increased pneumatic complexity in the latter (Figure 10). The trabecular architecture observed in *Majungasaurus* posterior cervical and anterior dorsal vertebrae resembles the "thick spongy" aspect of the camellate tissue described from the fortuitous breaks of the caudals of the brachyrostran abelisaurids *Kurupi* MPMA 27–0001/02 and Abelisauridae indet. MPM 99

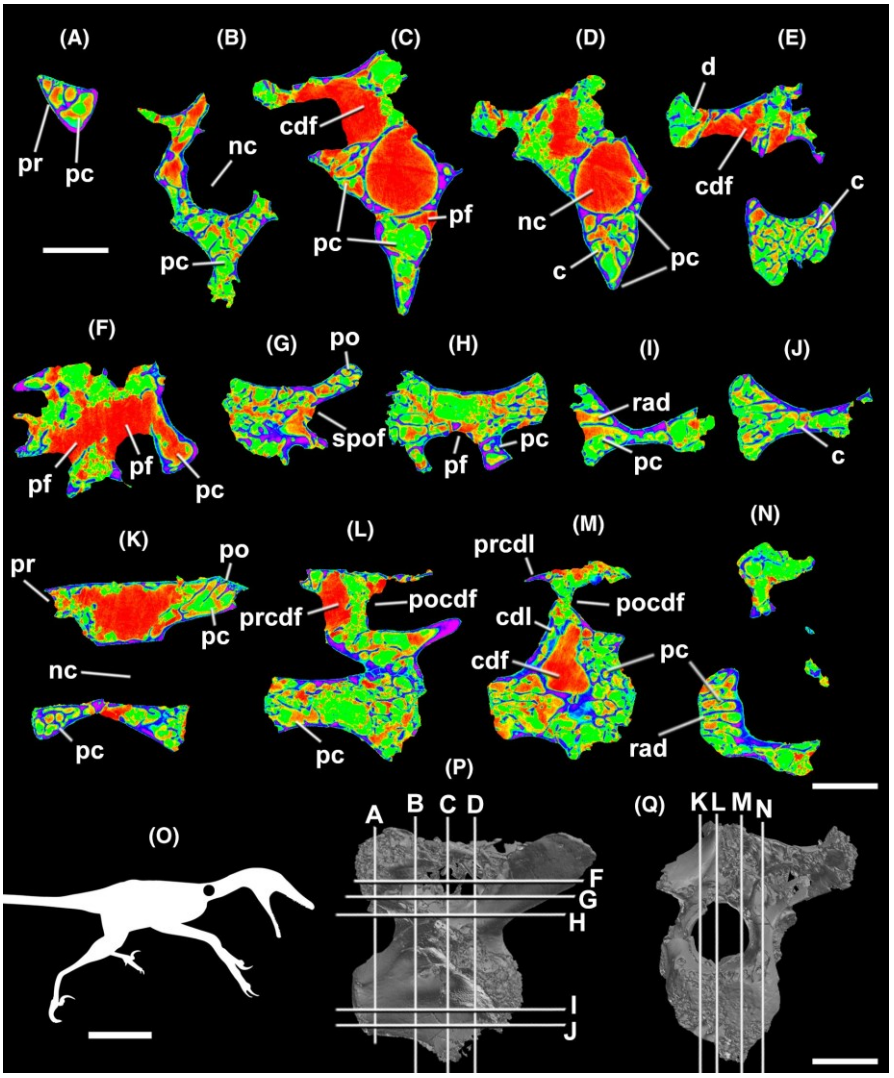

FIGURE 7 Micro-CT scan of *Rahonavis* (UA 8656) posterior cervical vertebra in transverse (A–E), frontal (F–J), and parasagittal (K–N) selected sections. (O) Silhouette shows the position of the axial element. Lighter blue and green indicate lower densities (e.g., pneumatic cavities). Purple and darker blue demonstrate denser structures (e.g., bone tissue). Red indicates either infilled sediments or empty spaces. Silhouette adapted from Jaime Headden (https://creativecommons.org/licenses/by-nc-sa/3.0/). Three-dimensional reconstruction of the vertebra and the correspondent slices in lateral (P) and proximal (Q) views. Scale bar = 10 mm.

(Baiano et al., 2023; Iori et al., 2021). The internal pneumatic signatures in the presacral series of the early avetheropodan *Allosaurus* UMNH-VP 10191 (Smith et al., 2021) remain similar to the condition observed in *Majungasaurus*, including apneumatic neural spines in the posterior cervical and dorsal elements. However, there is a noticeable decrease in density in the transverse processes and an enlargement of pneumatic foramina in the presacral series.

The internal traces of PSP in the posterior cervical and dorsal vertebrae of *Rahonavis* bear more similarities to the condition observed in the presacral elements of the maniraptoran therizinosaur *Nothronychus* AzMNH 2117 (Smith et al., 2021) and the bird *Mycteria americana* (USNM 18257; see Figure 10) than with the maniraptoriform ornithomimid *Archaeornithomimus* AMNH FARB 21788 (Watanabe et al., 2015). The anterior dorsal vertebrae of *Archaeornithomimus* demonstrate a decrease in pneumaticity compared with the polycamerate/camellate cervical elements within the same individual, with an almost entirely apneumatic tight trabecular matrix in the centra and apneumatic architecture inside the neural spine (as noted in *Allosaurus* and *Majungasaurus* posterior dorsals). Conversely, the cervical and dorsal vertebrae of *Nothronychus* present the complete pneumatization of the neural arch and the centrum.

Considering that *Majungasaurus* (a late abelisaurid) possibly inherited from their ceratosaurian ancestors, some internally apneumatic elements such as the dorsal neural spine and some centra, *Rahonavis* (an early paravian), demonstrated a different adaptation toward the full pneumatization of the axial skeleton (see Figure 10), an achievement that rendered paravians an advantage in gliding and flying. In sauropods, PSP traits configure broad chambers (camerae) in diplodocoids and delicate smaller chambers (camellae) in later titanosauriforms, demonstrating

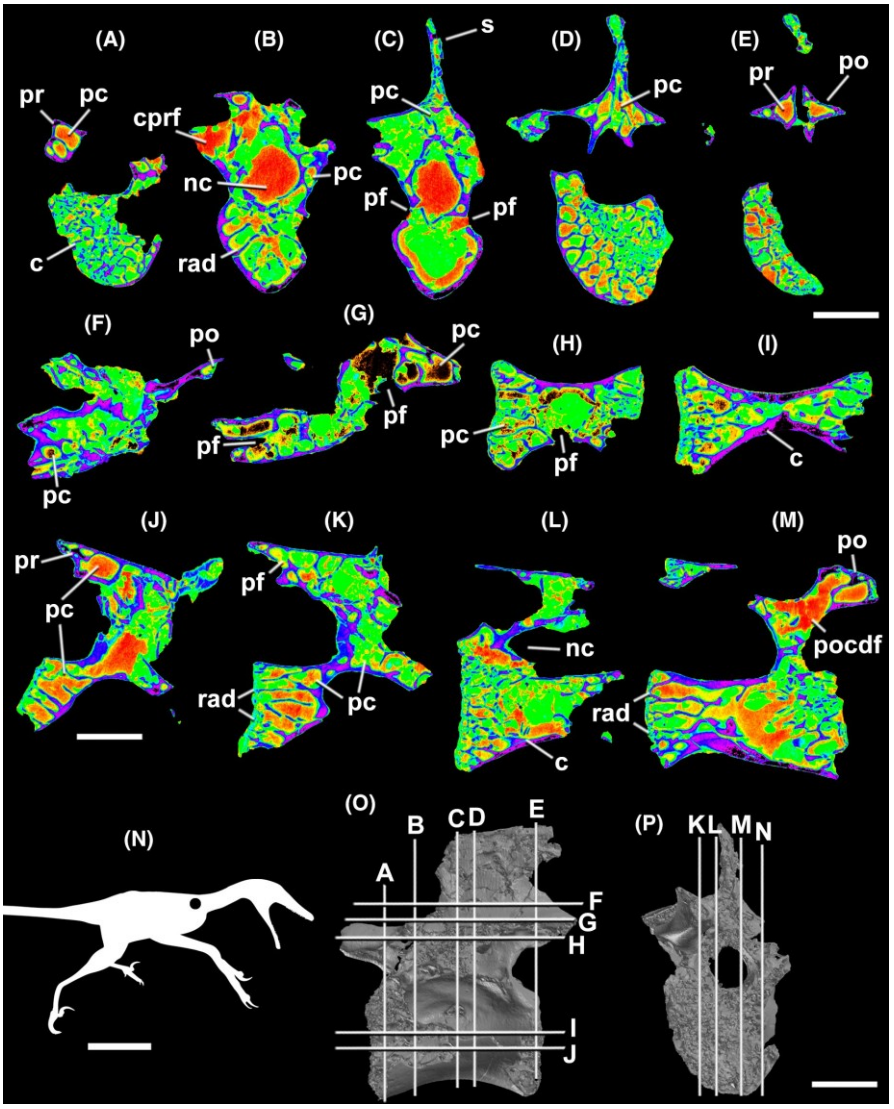

FIGURE 8 Micro-CT scan of *Rahonavis* (UA 8656) anterior dorsal vertebra (D1) in transverse (A–E), frontal (F–I), and parasagittal (J–M) selected sections. (N) Silhouette shows the position of the axial element. Lighter blue and green indicate lower densities (e.g., pneumatic cavities). Purple and darker blue demonstrate denser structures (e.g., bone tissue). Red indicates either infilled sediments or empty spaces. Silhouette adapted from Jaime Headden (https://creativecommons.org/licenses/by-nc-sa/3.0/). Three-dimensional reconstruction of the vertebra and the correspondent slices in lateral (O) and proximal (P) views. Scale bar = 10 mm.

a decrease in the chamber sizes in later neosauropods compared to early-diverging clades (Wedel, 2003, 2009). Unlike Sauropoda, current data on Theropoda suggest that the PSP in this group may have developed by increasing chamber volumes from early-diverging neotheropods toward early paravians (see Figure 10). Yet, this condition is not met in the therizinosaur *Nothronychus* AzMNH 2117 (Smith et al., 2021), which presents delicate camellate architectures equivalent to the structures described in saltasaurid titanosaurs (Aureliano et al., 2021; Cerda et al., 2012). This finding suggests that distinct patterns of PSP were present in maniraptorans (see Figure 10). Further tests are necessary to evaluate the effects of body mass, growth strategy, ecology, and phylogeny on the diversification of PSP in saurischians.

4.1 | Remarks on circumferential chambers

Circumferential chambers were found in some centra of *Majungasaurus* and *Rahonavis*, at the lateroventral borders of some cervical and dorsal elements. This is a condition shared with the sauropods *Apatosaurus* OMNH 01094 and *Ibirania* LPP-PV-0200 (Aureliano et al., 2021), the early non-massopodan sauropodomorphs *Buriolestes* CAPPA/UFSM 0035 and *Pampadromaeus* ULBRA-PV016, and the herrerasaurid *Gnathovorax* CAPPA/UFSM-0009 (Aureliano et al., 2022). The origins and function of this structure are still unknown. It is not related to PSP hence the occurrence in the non-pneumatized vertebrae of the early saurischians mentioned before. The circular bone architecture could offer structural resistance to the centrum and/or function as a deposit of fat and blood. It is advised to conduct a dissection in a modern analog

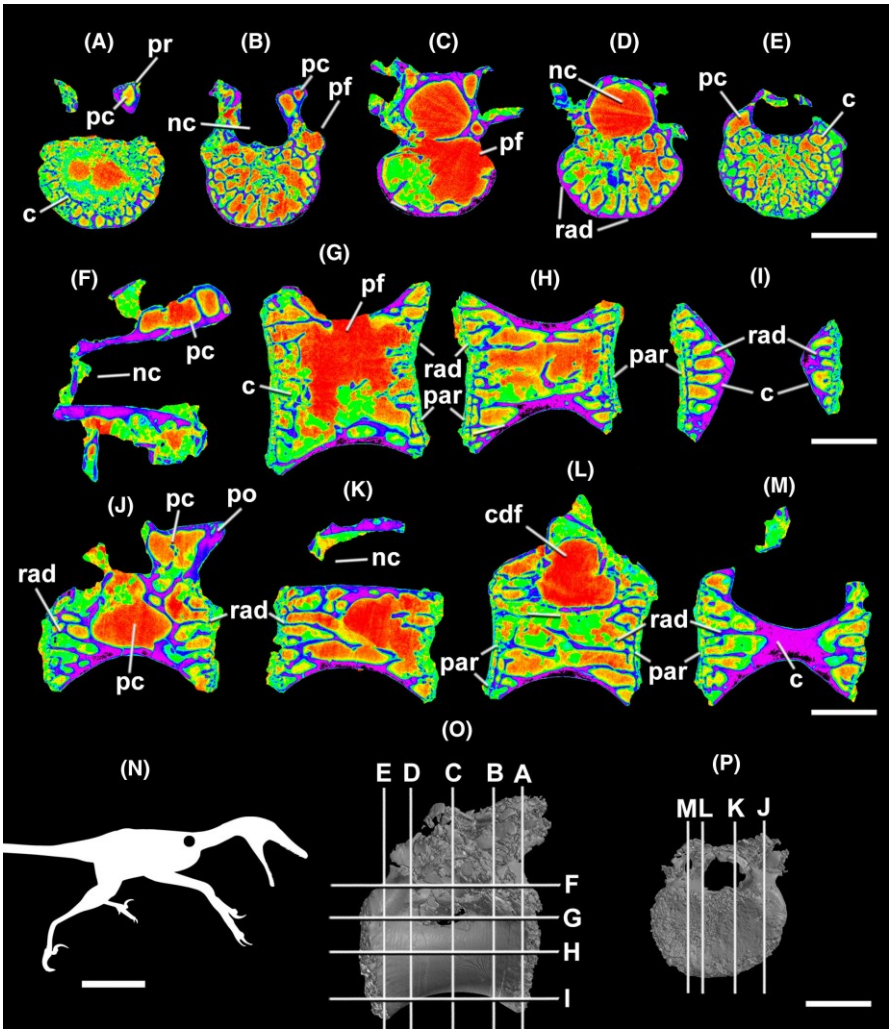

FIGURE 9 Micro-CT scan of *Rahonavis* (UA 8656) posterior dorsal vertebra in transverse (A–E), frontal (F–I), and parasagittal (J–M) selected sections. (N) Silhouette shows the position of the axial element. Lighter blue and green indicate lower densities (e.g., pneumatic cavities). Purple and darker blue demonstrate denser structures (e.g., bone tissue). Red indicates either infilled sediments or empty spaces. Silhouette adapted from Jaime Headden (https://creativecommons.org/licenses/by-nc-sa/3.0/). Three-dimensional reconstruction of the vertebra and the correspondent slices in lateral (O) and proximal (P) views. Scale bar = 10 mm.

vertebra to clarify these possibilities, in a taxon showing the same architecture on a CT scan.

4.2 | Observation on the two-layered trabeculae in the cotyle

A posterior dorsal centrum of *Rahonavis* shows two parallel layers of trabecular bone following the inner surface of the cotyles. This feature was observed in the dorsals of the early sauropodomorphs *Buriolestes* and *Pampadromaeus* (Aureliano et al., 2022), and the titanosaur *Ibirania* (Aureliano et al., 2021). Interestingly, this condition was not met throughout the presacral series of the non-coelurosaurian *Majungasaurus*. However, this structure is present in the sacral vertebrae of the ornithomimosaurian *Archaeornithomimus* AMNH FARB 21802 (Watanabe et al., 2015). This structure might be related either to the growth strategy or to the structural stability of the delicate nature of the thin trabecular arrangement in those organisms. Analyzing the effects of ontogeny in saurischians will be essential to solving this question (Aureliano et al., 2021).

4.3 | A warning for the evaluation of PSP based solely on the external morphology

The posterior dorsal centrum of *Majungasaurus* shows a lateral fossa ("pleurocoel"), but the CT scan revealed an apneumatic architecture (tight trabecular matrix) inside the element and no foramina connecting both of these structures. This dense trabecular arrangement is similar to the one described in the dorsal centra of *Dinornis* UCMP 77209 (Smith et al., 2021). Contrastingly, the neural arch in *Majungasaurus* is intensely pneumatized. This finding suggests that different pneumatizing organs were affecting the internal microarchitecture, and also suggests extra caution when interpreting skeletal pneumaticity

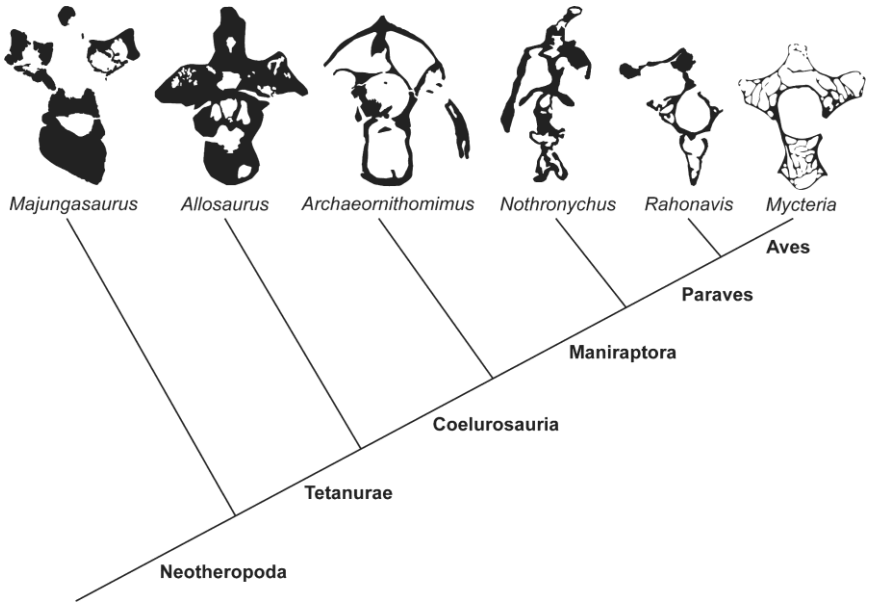

FIGURE 10 High-contrast transverse CT scan slices of posterior cervical vertebrae of theropod dinosaurs and their phylogenetic context. *Majungasaurus* (UA 8678), *Allosaurus* (UMNH-VP 10191; Smith et al., 2021), *Archaeornithomimus* (AMNH FARB 21802; Watanabe et al., 2015), *Nothronychus* (AzMNH 2117; Smith et al., 2021), *Rahonavis* (UA 8656; Forster et al., 2020), and *Mycteria* (USNM 1825; Andrew Moore provided access to these data, with data collection funded by NSF DGE-1246908 and data upload to MorphoSource funded by DBI-1902242. The files were downloaded from www.MorphoSource.org, Duke University). Not to scale.

traces solely based on macroscopic external features such as pleurocoels and fossae, since these alone could mislead the interpretation of unambiguous PSP. This same pattern of pneumatization was not observed in *Rahonavis* and indicates a variation in the soft-tissue air sac diverticular systems between distinct theropod clades.

5 | CONCLUSIONS

The description of the internal pneumatic traces present in the presacral series of *Majungasaurus* and *Rahonavis* brought new insights into the evolution of air sacs in theropod dinosaurs. Major finds are highlighted below:

- The CT scans revealed a greater pneumatic complexity in *Rahonavis* compared to *Majungasaurus*.
- *Majungasaurus* presents some apneumatic neural spine, a condition also observed in *Allosaurus*.
- *Majungasaurus* also displays some apneumatic centra despite the presence of lateral fossa. This raises caution when evaluating PSP solely based on external morphology.
- We found evidence of distinct patterns of PSP in maniraptorans.
- *Rahonavis* demonstrates that paravians evolved complete pneumatization of the axial skeleton early on in their evolutionary trajectory. This characteristic favored the evolution of flight within the group but was reversed in some taxa, possibly due to their ecology.

Finally, we conclude by stating that similar studies on early Theropoda from the Triassic and Jurassic will be essential to elucidate their conditions and infer possible evolutionary trends across clades.

AUTHOR CONTRIBUTIONS

TA conducted the CT scan densitometry analysis and provided the results. MR wrote on the geology context. TA, WA, and AMG provided a discussion on the evolution of the air sacs. All authors wrote and revised the manuscript.

ACKNOWLEDG MENTS

We acknowledge reviewers Guillermo Windholz and Virginia Zurriaguz from the Universidad Nacional de Rio Negro (Argentina) and Andrew Farke for their helpful insights on an earlier version of this study. The authors would like to thank the following funding agencies: Fundação Norte-Rio-Grandense de Pesquisa e Cultura (FUNPEC-UFRN/PIB21712-2023) (AMG) and Fundação Cearense de Apoio ao Desenvolvimento Científico e Tecnológico (FUNCAP/FPD-0213-00295.01.01/23) (TA). We thank Patrick M. O'Connor, Joseph Groenke and colleagues, who provided access to these data originally published in SVP Memoir 8 (2007, Vol. 27, Suppl. 2) and Foster et al. (2020) with data collection and processing funded by the US NSF EAR_9418816, NSF EAR_1123642, NSF EAR_1525915, NSF DBI_2242717, and Ohio University Heritage College of Osteopathic Medicine. The files were downloaded from www.MorphoSource.org, Duke University.

CONFLICT OF INTEREST STATEMENT

The authors declare no competing interests.

DATA AVAILABILITY STATEMENT

All fossils are housed in a research institution and can be accessed with a request from the collection's curator. Tomography data is available in Morphosource (links provided in Materials and Methods).

ORCID

Tito Aureliano https://orcid.org/0000-0002-6918-0519
Aline M. Ghilardi https://orcid.org/0000-0001-9136-0236

REFERENCES

Aranciaga Rolando, M., Garcia Marsà, J. & Novas, F. (2020) Histology and pneumaticity of *Aoniraptor libertatem* (Dinosauria, Theropoda), an enigmatic mid-sized megaraptoran from Patagonia. *Journal of Anatomy*, 237(4), 741–756.

Aureliano, T., Ghilardi, A.M., Müller, R.T., Kerber, L., Fernandes, M.A., Ricardi-Branco, F. et al. (2023) The origin of an invasive air sac system in sauropodomorph dinosaurs. *Anatomical Record*, 307, 1084–1092. Available from: https://doi.org/10.1002/ar.25209

Aureliano, T., Ghilardi, A.M., Müller, R.T., Kerber, L., Pretto, F.A., Fernandes, M.A. et al. (2022) The absence of an invasive air sac system in the earliest dinosaurs suggests multiple origins of vertebral pneumaticity. *Scientific Reports*, 12(1), 20844.

Aureliano, T., Ghilardi, A.M., Navarro, B.A., Fernandes, M.A., Ricardi-Branco, F. & Wedel, M.J. (2021) Exquisite air sac histological traces in a hyperpneumatized nanoid sauropod dinosaur from South America. *Scientific Reports*, 11(1), 24207.

Aureliano, T., Ghilardi, A.M., Silva-Junior, J.C.G., Martinelli, A.G., Ribeiro, L.C.B., Marinho, T. et al. (2020) Influence of taphonomy on histological evidence for vertebral pneumaticity in an upper Cretaceous titanosaur from South America. *Cretaceous Research*, 108, 104337.

Baiano, M.A., Coria, R., Chiappe, L.M., Zurriaguz, V. & Coria, L. (2023) Osteology of the axial skeleton of *Aucasaurus garridoi*: phylogenetic and paleobiological inferences. *PeerJ*, 11, e16236.

Besairie, H. (1969) "Carte géologique [Majunga, No3]. 1: 500,000." Service Géologique de Madagasikara.

Britt, B.B. (1994) Pneumatic postcranial bones in dinosaurs and other archosaurs. https://elibrary.ru/item.asp?id=5724623

Britt, B.B., Makovicky, P.J., Gauthier, J. & Bonde, N. (1998) Postcranial pneumatization in archaeopteryx. *Nature*, 395(6700), 374–376.

Brum, A.S., Machado, E.B., de Almeida Campos, D. & Kellner, A.W.A. (2018) Description of uncommon pneumatic structures of a noasaurid (Theropoda, Dinosauria) cervical vertebra from the Bauru group (upper Cretaceous), Brazil. *Cretaceous Research*, 85, 193–206.

Cerda, I.A., Salgado, L. & Powell, J.E. (2012) Extreme postcranial pneumaticity in sauropod dinosaurs from South America. *Paläontologische Zeitschrift*, 86(4), 441–449.

Cuesta, E., Díaz-Martínez, I., Ortega, F. & Sanz, J.L. (2015) Did all theropods have chicken-like feet? First evidence of a non-avian dinosaur podotheca. *Cretaceous Research*, 56, 53–59.

Fanti, F. & Therrien, F. (2007) Theropod tooth assemblages from the late Cretaceous Maevarano formation and the possible presence of dromaeosaurids in Madagascar. *Acta Palaeontologica Polonica*, 52(1), 155–166.

Fedorov, A., Beichel, R., Kalpathy-Cramer, J., Finet, J., Fillion-Robin, J.-C., Pujol, S. et al. (2012) 3D slicer as an image computing platform for the quantitative imaging network. *Magnetic Resonance Imaging*, 30(9), 1323–1341.

Forster, C.A., O'Connor, P.M., Chiappe, L.M. & Turner, A.H. (2020) The osteology of the late Cretaceous paravian *Rahonavis ostromi* from Madagascar. *Palaeontologia Electronica*, 23(2), a29. Available from: https://doi.org/10.26879/793

Forster, C.A., Sampson, S.D., Chiappe, L.M. & Krause, D.W. (1998a) Genus correction. *Science*, 280(5361), 179.

Forster, C.A., Sampson, S.D., Chiappe, L.M. & Krause, D.W. (1998b) The theropod ancestry of birds: new evidence from the late Cretaceous of Madagascar. *Science*, 279(5358), 1915–1919.

Gianechini, F.A. & Zurriaguz, V.L. (2021) Vertebral pneumaticity of the paravian theropod *Unenlagia comahuensis*, from the upper Cretaceous of Patagonia, Argentina. *Cretaceous Research*, 104925, 104925.

Iori, F.V., de Araújo-Júnior, H.I., Tavares, S.A.S., Marinho, T.d.S. & Martinelli, A.G. (2021) New theropod dinosaur from the late Cretaceous of Brazil improves abelisaurid diversity. *Journal of South American Earth Sciences*, 112, 103551.

Krause, D.W., O'Connor, P.M., Sertich, J.J.W., Curry Rogers, K., Rogers, R.R. & Rakotozafy, B. (2022) Late Cretaceous vertebrates of Madagascar: a window into Gondwanan biogeography at the end of the age of dinosaurs. In: Goodman, S.M. & Andrianarimisa, A. (Eds.) *The new natural history of Madagascar*. Princeton, NJ: Princeton University Press, pp. 59–68.

Krause, D.W., Sampson, S.D., Carrano, M.T. & O'Connor, P.M. (2007) Overview of the history of discovery, taxonomy, phylogeny, and biogeography of *MAJUNGASAURUS CRENATISSIMUS* (THEROPODA: ABELISAURIDAE) from the late CRETACEOUS of Madagascar. *Journal of Vertebrate Paleontology*, 27(sup2), 1–20.

Lavocat, R. (1955) Sur une portion de mandibule de Théropode provenant du Crétacé supérieur de Madagascar. *Bulletin Du Muséum National d'Histoire Naturelle*, 27, 256–259.

Maina, J. (2005) *The lung-air sac system of birds: development, structure, and function*. Berlin: Springer Science & Business Media.

Maina, J.N. (2006) Development, structure, and function of a novel respiratory organ, the lung-air sac system of birds: to go where no other vertebrate has gone. *Biological Reviews of the Cambridge Philosophical Society*, 81(4), 545–579.

Malafaia, E., Gasulla, J.M., Escaso, F., Narváez, I., Sanz, J.L. & Ortega, F. (2018) New spinosaurid (Theropoda, Megalosauroidea) remains from the Arcillas de Morella formation (upper Barremian) of Morella, Spain. *Cretaceous Research*, 92, 174–183.

Müller, R.T. (2021) A new theropod dinosaur from a peculiar late Triassic assemblage of southern Brazil. *Journal of South American Earth Sciences*, 107, 103026.

O'Connor, J. & Zhou, Z. (2015) Early evolution of the biological bird: perspectives from new fossil discoveries in China. *J Ornithology*, 156(1), 333–342.

O'Connor, P.M. (2006) Postcranial pneumaticity: an evaluation of soft-tissue influences on the postcranial skeleton and the reconstruction of pulmonary anatomy in archosaurs. *Journal of Morphology*, 267(10), 1199–1226.

O'Connor, P.M. (2007) The postcranial axial skeleton of *Majungasaurus cretanissimus* (Theropoda: Abelisauridae) from the late Cretaceous of Madagascar. *Journal of Vertebrate Paleontology*, 27(sup2), 127–163.

Poropat, S.F., Pentland, A.H., Duncan, R.J. & Bevitt, J.J. (2020) First elaphrosaurine theropod dinosaur (Ceratosauria: Noasauridae) from Australia—a cervical vertebra from the early Cretaceous of Victoria. *Gondwana Research* https://www.sciencedirect.com/science/article/pii/S1342937X20301234?casa_token=av5Q8XBvx6EAAAAA:AKYSWJlvyAAH_cwiZIVxaNGcaY0xjLBqP2baxYqtZkp8QearD3kD5kdct5r4NrCOEdANUZsoKZ4, 84, 284–295.

Proctor, N.S. & Lynch, P.J. (1993) *Manual of ornithology: avian structure & function*. New Haven, CT: Yale University Press.

Rayfield, E.J. (2005) Aspects of comparative cranial mechanics in the theropod dinosaurs Coelophysis, allosaurus and tyrannosaurus. *Zoological Journal of the Linnean Society*, 144(3), 309–316.

Rogers, R.R., Hartman, J.H. & Krause, D.W. (2000) Stratigraphic analysis of upper Cretaceous rocks in the Mahajanga Basin, northwestern Madagascar: implications for ancient and modern faunas. *The Journal of Geology*, 108(3), 275–301.

Sampson, S.D. & Witmer, L.M. (2007) Craniofacial anatomy of *MAJUNGASAURUS CRENATISSIMUS* (THEROPODA: ABELISAURIDAE) from the late CRETACEOUS of Madagascar. *Journal of Vertebrate Paleontology*, 27(sup2), 32–104.

Smith, D.K., Sanders, R.K. & Wolfe, D.G. (2021) Vertebral pneumaticity of the north American therizinosaur *Nothronychus*. *Journal of Anatomy*, 238(3), 598–614.

Taylor, M. & Wedel, M. (2021) Why is vertebral pneumaticity in sauropod dinosaurs so variable? *Qeios*, 1G6J3Q. Available from: https://doi.org/10.32388/1g6j3q

Watanabe, A., Eugenia Leone Gold, M., Brusatte, S.L., Benson, R.B.J., Choiniere, J., Davidson, A. et al. (2015) Vertebral Pneumaticity in the Ornithomimosaur *Archaeornithomimus* (Dinosauria: Theropoda) revealed by computed tomography imaging and reappraisal of axial Pneumaticity in Ornithomimosauria. *PLoS One*, 10(12), e0145168.

Wedel, M.J. (2003) Vertebral pneumaticity, air sacs, and the physiology of sauropod dinosaurs. *Paleobiology*, 29(2), 243–255.

Wedel, M.J. (2007) What pneumaticity tells us about "prosauropods", and vice versa. *Special Papers in Palaeontology*, 77, 207–222.

Wedel, M.J. (2009) Evidence for bird-like air sacs in saurischian dinosaurs. *Journal of Experimental Zoology. Part A, Ecological Genetics and Physiology*, 311(8), 611–628.

Wedel, M.J., Cifelli, R.L. & Sanders, R.K. (2000) Osteology, paleobiology, and relationships of the sauropod dinosaur *Sauroposeidon*. *Acta Palaeontologica Polonica*, 45(4), 343–388. http://yadda.icm.edu.pl/yadda/element/bwmeta1.element.agro-article-46c7b594-4a8b-476d-aa1c-4c117ed1f8fa/c/app45-343.pdf

Wilson, J.A. (1999) A nomenclature for vertebral laminae in sauropods and other saurischian dinosaurs. *Journal of Vertebrate Paleontology*, 19(4), 639–653.

Wilson, J.A. (2012) New vertebral laminae and patterns of serial variation in vertebral laminae of sauropod dinosaurs. https://deepblue.lib.umich.edu/bitstream/handle/2027.42/92460/Contributions32no7-HR-c08-15-2012.pdf?sequence=2

Wilson, J.A., D'Emic, M.D., Ikejiri, T., Moacdieh, E.M. & Whitlock, J.A. (2011) A nomenclature for vertebral fossae in sauropods and other saurischian dinosaurs. *PLoS One*, 6(2), e17114.

Zanno, L.E. & Makovicky, P.J. (2011) Herbivorous ecomorphology and specialization patterns in theropod dinosaur evolution. *Proceedings of the National Academy of Sciences of the United States of America*, 108(1), 232–237.

How to cite this article: Aureliano, T., Almeida, W., Rasaona, M. & Ghilardi, A.M. (2024) The evolution of the air sac system in theropod dinosaurs: Evidence from the Upper Cretaceous of Madagascar. *Journal of Anatomy*, 00, 1–13. Available from: https://doi.org/10.1111/joa.14113